J. Fluid Mech. (1969), *vol.* 38, *part* 3, *pp.* 433–455
Printed in Great Britain

Axisymmetric turbulent mass transfer in a circular tube

By ALAN QUARMBY
The University of Manchester Institute of Science and Technology
AND R. K. ANAND
Indian Institute of Technology, Delhi

(Received 22 July 1968)

Solutions of the diffusion equation are obtained for mass transfer in a fully developed turbulent flow in a plain circular tube in two axisymmetric situations. The cases studied are a point source positioned at the centre of the tube and a ring source in the tube wall in which there is a uniform mass flux along a short length of the tube. The purpose of the work is to establish the correctness of the descriptions of the velocity profile and radial eddy diffusivities of mass and momentum in order to provide a firm base from which consideration of the non-axisymmetric situation could proceed.

The turbulent velocity profile is deduced from a two-part model based on a sublayer profile and the Von Kármán similarity hypothesis. The radial eddy diffusivity of momentum is described by an expression due to Reichardt and Van Driest and from this the radial eddy diffusivity of mass as a function of radius is obtained by use of a ratio which takes account of fluid properties and the value of the radial eddy diffusivity.

The analysis is substantiated by experiments carried out with nitrous oxide, Schmidt number = 0·77, for Reynolds numbers from 20,000 to 130,000. The concentration profiles measured at several axial positions downstream from the source are in good agreement with the analytical solutions in both cases. Direct measurements of the eddy diffusivity of mass and momentum were obtained as added confirmation and also gave good agreement with the theory.

1. Introduction

The problem of turbulent heat and mass transfer in a plain tube has received considerable attention both analytically and experimentally. The bulk of the work on this problem has been confined to fully developed flow with axisymmetric boundary conditions. Situations, in which there are circumferential variations in the heat or mass flux, or tangential variations of temperature or concentration, have been relatively neglected. Such cases are, however, very common in practice.

An analysis of the non-axisymmetric situation would require a knowledge of the diffusion process in the tangential direction as well as in the radial direction. The most useful information, which might be obtained, is the relationship which may exist between the tangential eddy diffusivity ϵ_ω and the radial eddy diffusivity ϵ_r. The accuracy of the results, which could be obtained for ϵ_ω, would

depend very much on having an accurate description of the radial eddy diffusivity and velocity profile. The literature on axisymmetric heat or mass transfer to a fully developed turbulent flow in a plain tube is extensive. There is some disagreement, however, about which description of the velocity profile or radial eddy diffusivity best fits the experimental measurements.

Experimentally, it is easier to ensure a precisely defined boundary condition, either axisymmetric or otherwise, with mass transfer than it is with heat transfer. The diffusion of nitrous oxide gas at low concentrations in air provides an experimental situation, in which the eddy diffusivities of mass in both the radial and tangential directions may be studied. Further, the analogy between heat and mass transfer is probably better than that between heat and momentum transfer, since heat and mass are both scalar quantities. The analogy between heat and momentum is valid only for uni-directional flow. Conclusions drawn from the mass transfer situation should be very relevant to the heat transfer situation. Experimental work for mass transfer is rather less extensive than for heat transfer; although, since the governing equations are identical, the theoretical results and the assumptions, on which they are based, should be valid in both cases.

In some of the work on heat transfer in a plain tube (e.g. Sparrow, Hallman & Seigel 1957), the eddy diffusivity of momentum $\epsilon_{m,r}$ was derived from the velocity profile, and the radial eddy diffusivity of heat $\epsilon_{h,r}$ taken equal to $\epsilon_{m,r}$. The value of $\epsilon_{m,r}$ and $\epsilon_{h,r}$ thus obtained is -1 at the centre of the tube. This may be passable for symmetric cases, but it is clearly wrong if there is heat transfer across the centre of the tube or other duct, due to asymmetry of the boundary conditions. Thus, for an annulus with heat fluxes, which were not equal at the two walls, Leung, Kays & Reynolds (1962) formulated the velocity profile to give the best fit with experimental evidence. The eddy diffusivity of momentum was described separately by means of the same criterion, and was not consistent with the velocity description. The radial eddy diffusivity of heat was then obtained from $\epsilon_{m,r}$ by the use of a ratio due to Jenkins (1951), which takes account of the value of $\epsilon_{m,r}$ and of the Prandtl number of the fluid.

Investigations of axisymmetric mass transfer in a plain tube have been carried out by Schlinger & Sage (1953), Towle & Sherwood (1939) and Sherwood & Woertz (1939). In each of these, the radial eddy diffusivity of mass $\epsilon_{d,r}$ was taken as a constant. No consideration was given to the variation of $\epsilon_{d,r}$ with distance from the wall. This is clearly an oversimplification.

Taylor (1954) considered dispersion in turbulent flow in a pipe and assumed a universal velocity profile, from which the radial eddy diffusivity of momentum was obtained. Thus, according to Taylor, the velocity u in the direction x of the axis of the tube of radius r_0 is given at any radius r by

$$(u_c - u)/u^* = f(z), \tag{1}$$

where $z = r/r_0$, and u_c is the velocity at the centre of the tube. The friction velocity u^* is $\sqrt{(\tau_0/\rho)}$, where τ_0 is the wall shear and ρ the density of the fluid. The eddy diffusivity of momentum is given by

$$\epsilon_{m,r} = r_0 u^* z/f'(z), \tag{2}$$

where $f'(z) = df(z)/dz$. Taylor put $\epsilon_{d,r}$ equal to $\epsilon_{m,r}$ by Reynolds analogy. In Taylor's work no account was taken of a sublayer velocity profile. There was no direct experimental support for Taylor's calculations of the eddy diffusivity of mass, and the validity of the universal velocity profile $f(z)$ is challengeable.

Clearly, there is a lack of agreement in previous work on the correct description of the velocity profile and $\epsilon_{m,r}$, and or how $\epsilon_{h,r}$ is related to $\epsilon_{m,r}$ in heat transfer, or $\epsilon_{d,r}$ to $\epsilon_{m,r}$ in mass transfer. Since the results for the tangential eddy diffusivity of mass $\epsilon_{d,\omega}$ depend very much on the accuracy of the expressions used for the velocity profile and radial eddy diffusivity of mass, it was considered essential to investigate axisymmetric mass transfer, and establish firm conclusions concerning these quantities, before dealing with the non-axisymmetric situation.

2. Analysis and formulation of the equations

(i) *The diffusion equation*

Solutions of the diffusion equation were sought for two cases, in which mass transfer occurs from a specified axisymmetric boundary condition into a fully developed turbulent flow in a plain tube. The two cases studied were: (*a*) axisymmetric diffusion from a point source in the centre of the tube, (*b*) axisymmetric diffusion from a ring source in the wall of the tube.

These two cases were chosen, because in (*a*) the initial diffusion occurs mainly in the centre of the tube, where there is some evidence from hot wire anemometry to suggest that the turbulence is isotropic, whilst in (*b*) it occurs initially through the anisotropic sublayer. The correct description of the velocity in the sublayer is different from that of the velocity outside the sublayer in the centre of the tube. It was considered necessary to treat both these cases, since a satisfactory agreement between theory and experiment for only the one case would not be enough to allow conclusions to be drawn about the other with certainty.

The governing differential equation of the concentration c, at any radius r and axial distance x, is given by

$$u\frac{\partial c}{\partial x} = \frac{1}{r}\frac{\partial}{\partial r}\left[r(D+\epsilon_{d,r})\frac{\partial c}{\partial r}\right], \tag{3}$$

where D is the molecular diffusivity. This equation contains the usual assumptions of steady-state conditions, constant fluid properties and negligible axial diffusion. It is put in non-dimensional form by the following substitutions

$$\theta = \frac{c}{c_m}, \quad x^+ = \frac{x}{r_0}, \quad r^+ = \frac{ru^*}{\nu},$$

$$r_0^+ = \frac{r_0 u^*}{\nu} \quad \text{and} \quad u^+ = \frac{u}{u^*},$$

where ν is the kinematic viscosity of the fluid, and the bulk mean concentration c_m is given by

$$c_m = \int_0^{r_0} cur\,dr \Big/ \int_0^{r_0} ur\,dr. \tag{4}$$

Thus, (3) becomes

$$u^+\frac{\partial\theta}{\partial x^+} = \frac{r_0^+}{r^+}\frac{\partial}{\partial r^+}\left[r^+\left(\frac{1}{S}+\frac{\epsilon_{d,r}}{\nu}\right)\frac{\partial\theta}{\partial r^+}\right], \tag{5}$$

in which S is the Schmidt number ν/D.

If the initial concentration profile at $x^+ = 0$ is denoted θ_i, then the boundary conditions on (5) for the impermeable wall are

$$\theta(0, r_0^+) = \theta_i, \tag{6}$$

and
$$\partial\theta/\partial r^+ = 0 \quad \text{at} \quad r^+ = r_0^+ \quad \text{for all} \quad x^+, \tag{7a}$$

and
$$\partial\theta/\partial r^+ = 0 \quad \text{at} \quad r^+ = 0 \quad \text{for all} \quad x^+. \tag{7b}$$

Since (5) is linear, the concentration may be expressed as the sum of a fully developed part θ_1, which is independent of x^+, and a developing part θ_2. It is clear that, since the wall is impermeable, the concentration profile for large x^+ will be uniform. That is,

$$\theta = \theta_i = 1. \tag{8}$$

A variables separable solution of the form

$$\theta_2 = \phi(r^+)\,\psi(x^+)$$

is sought for the developing part. It is easily shown that

$$\psi = \exp\left[\frac{-2\beta_n^2 x^+}{R}\right], \tag{9}$$

where the Reynolds number R, is defined by

$$R = \frac{2r_0 u_m}{\nu},$$

and
$$u_m = \frac{2}{r_0^2}\int_0^{r_0} ur\,dr. \tag{10}$$

The eigenvalues β_n^2 and eigenfunctions ϕ_n are given by

$$\frac{d}{dr^+}\left[r^+\left(\frac{1}{S}+\frac{\epsilon_{d,r}}{\nu}\right)\frac{d\phi_n}{dr^+}\right] + \frac{2\beta_n^2 u^+ r^+ \phi_n}{Rr_0^+} = 0, \tag{11}$$

with boundary conditions

$$\phi(0, r^+) = \theta_i - 1 \tag{12}$$

and
$$d\phi/dr^+ = 0 \quad \text{at} \quad r^+ = r_0^+ \quad \text{for all} \quad x^+, \tag{13a}$$

and
$$d\phi/dr^+ = 0 \quad \text{at} \quad r^+ = 0 \quad \text{for all} \quad x^+. \tag{13b}$$

The solution for θ_2 is thus

$$\theta_2 = \sum_{n=1}^{n=\infty} C_n\phi_n \exp\left(\frac{-2\beta_n^2 x^+}{R}\right), \tag{14}$$

where
$$C_n = \frac{\displaystyle\int_0^{r_0^+} (1-\theta_i)\,\phi_n u^+ r^+\,dr^+}{\displaystyle\int_0^{r_0^+} u^+ r^+ \phi_n^2\,dr^+}, \tag{15}$$

from the Sturm–Liouville condition. The non-dimensional concentration θ is given at any point downstream of the source by

$$\theta = \theta_1 + \theta_2,$$
$$= 1 + \sum_{n=1}^{n=\infty} C_n \phi_n \exp\left(\frac{-2\beta_n^2 x^+}{R}\right). \tag{16}$$

(ii) *Initial concentration profile*

The above equations hold for both the cases studied if the position $x^+ = 0$ is taken at the point source in the first case, or at the downstream edge of the ring source in the second case. The difference between the two cases arises in evaluating the constants C_n from the initial profile θ_i by (15). Evaluating C_n for a point source is difficult, since the corresponding θ_i is discontinuous. It is easier, mathematically, to take θ_i for the point source as the measured concentration profile at a short distance downstream of the source. This procedure has a further advantage in the experimental situation, in that θ_i may be determined at some point downstream of the source, where disturbances to the velocity profile due to the presence of the source in the stream have become negligible.

The second case has the advantage that the ring source is flush with the tube wall, and there are no disturbances to the velocity profile. If θ_i is measured at the downstream edge of the ring source, the above solution is valid for all x^+ in the impermeable tube. Alternatively, another solution may be found by use of superposition of the solution for a uniform wall mass flux, which avoids measurement of θ_i. Thus, if x^+ is measured from the upstream edge of the ring source, which has length x_1^+, then $\theta_i = 0$, and the solution is as follows. A comparison between the two solutions for the ring source establishes the validity of taking θ_i as a measured concentration profile and the accuracy of the measurements and of the equation used for θ_i.

(iii) *Alternative solution for the ring source*

The concentration c is made non-dimensional by substituting $H = (c - c_i)/(Jr_0/D)$, where J is the mass flux per unit area, and c_i is the initial concentration at $x^+ = 0$.

Using the same non-dimensional variables as above, (3) then becomes

$$u^+ \frac{\partial H}{\partial x^+} = \frac{r_0^+}{r^+} \frac{\partial}{\partial r^+}\left[r^+ \left(\frac{1}{S} + \frac{\epsilon_{d,r}}{\nu}\right) \frac{\partial H}{\partial r^+}\right]. \tag{17}$$

The solution of (17) is written as a fully developed part H_1 and a developing part H_2. The solution for H_1 is

$$H_1 = \frac{4}{RS} x^+ + G(r^+), \tag{18}$$

where the first term follows from a simple mass balance, and $G(r^+)$ is given by the integration of

$$\frac{d}{dr^+}\left[r^+ \left(\frac{1}{S} + \frac{\epsilon_{d,r}}{\nu}\right) \frac{dG}{dr^+}\right] - \frac{4u^+ r^+}{RSr_0^+} = 0. \tag{19}$$

The boundary conditions on (19) are

$$G(0, r^+) = 0, \tag{20}$$

$$dG/dr^+ = 0 \quad \text{at} \quad r^+ = 0 \quad \text{for all} \quad x^+ \tag{21a}$$

$$dG/dr^+ = 1/r_0^+ \quad \text{at} \quad r^+ = r_0^+ \quad \text{for all } x^+. \tag{21b}$$

The developing part H_2 is again given by a variables separable solution as

$$H_2 = \sum_{n=1}^{n=\infty} B_n \phi_n \exp\left(\frac{-2\beta_n^2}{R} x^+\right), \tag{22}$$

where the eigenfunctions and eigenvalues are identical to those pertaining to (11). The constants, however, are given by

$$B_n = \frac{\int_0^{r_0^+} -u^+ r^+ G(r^+)\, \phi_n\, dr^+}{\int_0^{r_0^+} u^+ r^+ \phi_n^2\, dr^+}, \tag{23}$$

where use is made of the fact that $H = 0$ at $x^+ = 0$.

For values of $x^+ < x_1^+$ the concentration is given by the sum of H_1 and H_2. The solution for $x^+ > x_1^+$ is found by the addition of the solution for a uniform mass influx J in $x^+ > 0$, and the solution for an equal but opposite mass efflux $-J$ in $x^+ > x_1^+$. Thus, for the impermeable section of the tube

$$H = \frac{4}{RS} x_1^+ + \sum_{n=1}^{n=\infty} B_n \phi_n \left[\exp\left(\frac{-2\beta_n^2 x^+}{R}\right) - \exp\left(\frac{-2\beta_n^2 (x^+ - x_1^+)}{R}\right)\right], \tag{24}$$

and

$$\theta = 1 + \frac{RS}{4x_1^+} \sum_{n=1}^{n=\infty} B_n \phi_n \left[\exp\left(\frac{-2\beta_n^2 x^+}{R}\right) - \exp\left(\frac{-2\beta_n^2 (x^+ - x_1^+)}{R}\right)\right]. \tag{25}$$

(iv) *Description of the velocity profile*

In order to integrate (11), (15), (19), (23) a description of the velocity profile u^+ as a function of r^+ is required. Many such descriptions for fully developed turbulent flow in a tube have been proposed. In the present work, a two-part model is used, consisting of a sublayer close to the wall, for which $0 < y^+ < y_l^+$, and a mainstream outside of the sublayer, for which $y_l^+ < y^+ < y_0^+$. Here $y^+ = r_0^+ - r^+$, and the non-dimensional distance from the wall to the centre of the tube is consequently $y_0^+ = r_0^+$, and y_l^+ is the sublayer thickness. The validity of such a model is well established. In the sublayer, u^+ is given by integrating Deissler's (1955) expression

$$\frac{du^+}{dy^+} = \frac{1 - y^+/r_0^+}{1 + n^2 u^+ y^+ [1 - \exp(-n^2 u^+ y^+)]}, \tag{26}$$

with the boundary condition that $u^+ = 0$ at $y^+ = 0$.

This expression is derived from an eddy diffusivity of momentum expression given by

$$\frac{\epsilon_{m,r}}{\nu} = n^2 u^+ y^+ [1 - \exp(-n^2 u^+ y^+)], \tag{27}$$

where n^2 is a constant. Equation (27) is based on dimensional analysis, and the term in the brackets is chosen as the simplest expression, which fits the physical

arguments that the eddy diffusivity must be zero immediately adjacent to the wall, but approach the value n^2uy for higher levels of turbulence. It also fulfils the criterion given by Elrod (1957) that $\epsilon_{m,r}$ must be proportional to y^+ raised to a power not less than four, which is derived from consideration of the continuity equation applied to the fluctuating components of velocity very near to the wall. The success of this expression in predicting heat transfer at high Prandtl numbers has confirmed its superiority over earlier expressions.

In the mainstream, the velocity is obtained from Von Kármán's (1930) similarity hypothesis, so that the total shear stress τ is given by

$$\tau = \left(\mu + \rho l^2 \left|\frac{du}{dy}\right|\right)\frac{du}{dy}, \tag{28a}$$

where the effect of molecular viscosity μ is taken into account, and

$$l = K\frac{du}{dy}\Big/\frac{d^2u}{dy^2}, \tag{28b}$$

where l is the mixing length and K a constant. Integration of (28), and use of a linear shear stress variation across the tube, gives the expression for u in the mainstream as

$$\frac{d^2u^+}{dy^{+2}} = -\frac{K(du^+/dy^+)^2}{\left[\left(1-\frac{y^+}{r_0^+}\right)-\frac{du^+}{dy^+}\right]^{\frac{1}{2}}}, \tag{29}$$

and the boundary conditions on (29) are that at y_l^+ the slope and ordinate of u^+ are equated to the corresponding values resulting from integration of the sublayer profile.

The velocity profile given by (26), (29) does not have some of the faults which are present in velocity profiles used in previous work. For example, there are no discontinuities in the velocity gradient at the edge of the sublayer, and the correct centre-line boundary condition that $du^+/dy^+ = 0$ at y_0^+ is fulfilled. In (29) the index n^2 was determined by Deissler (1955) as 0·0154. Quarmby (1969) has shown that n^2, which accounts for the effect of the wall on the turbulence, and the sublayer thickness y_l^+, are functions of the flow. The relationship between n^2 and r^+, and between y_0^+ and R, which was deduced by Quarmby, is shown in figure 1. For the Von Kármán similarity hypothesis, the constant K was taken as 0·36. This formulation of the equations of the velocity profile applies equally well to both the plain tube and parallel plate channel, and correctly describes the Reynolds number dependence of the $u^+ \sim y^+$ correlation in both configurations. The satisfactory agreement between theory and experiment holds for Reynolds numbers from 6000 to 400,000.

(v) *Description of the radial eddy diffusivity of momentum*

The equations for the velocity in the mainstream could be used to give a description of $\epsilon_{m,r}$ in that region from the expression

$$\epsilon_{m,r} = l^2\left|\frac{du}{dy}\right|. \tag{30}$$

However, the value of $\epsilon_{m,r}$ thus obtained is zero at y_0^+. This is not in agreement with experiment; further, it is not acceptable, because it would predict a zero value for $\epsilon_{d,r}$ at y_0^+, if $\epsilon_{d,r}$ is obtained from $\epsilon_{m,r}$ by some expression for their ratio. Accordingly, the radial eddy diffusivity of momentum is described by an expression based on the work of Van Driest (1956) and Reichardt (1951).

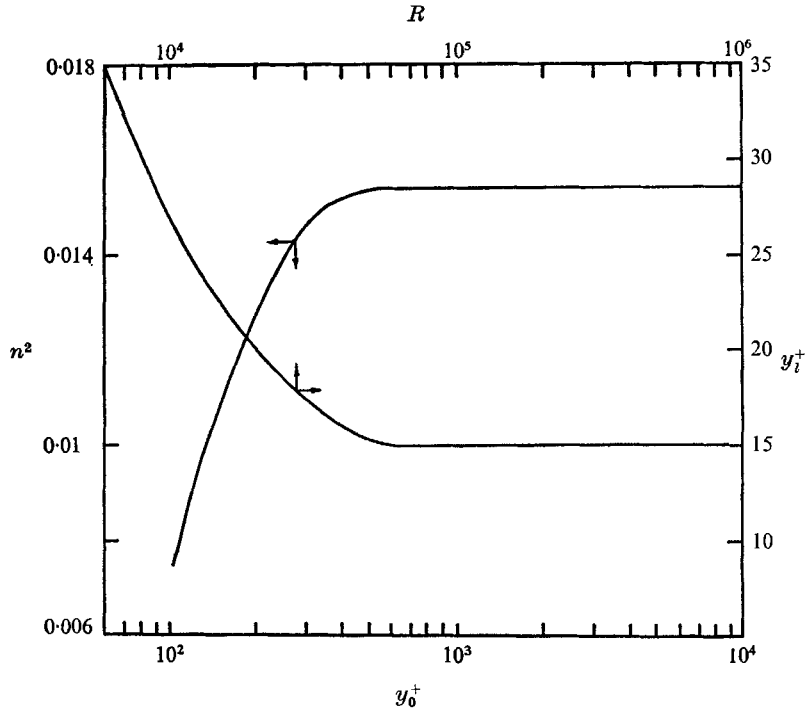

FIGURE 1. Relationship between the parameters of the velocity profile.

Van Driest considered that near the wall the shear stress is given by (28*a*), whilst the mixing length for fully turbulent flow away from the wall, as given by Prandtl (1933), is

$$l = Ky. \tag{31}$$

The effect of the wall on the turbulent fluctuations is estimated from Stokes' (1851) solution for an infinite flat plate undergoing simple harmonic motion in a infinite fluid. By analogy with Stokes' solution, the velocity fluctuation near the wall is damped by a factor $[1-\exp(-y/A)]$, where A is a constant depending on the frequency of oscillation and ν. The Prandtl mixing length is multiplied by this factor to give

$$\tau = \frac{dy}{du} + K^2y^2\left[1-\exp\left(-\frac{y}{A}\right)\right]^2\left(\frac{du}{dy}\right)^2. \tag{32}$$

By definition,

$$\epsilon_{m,r} = \frac{\tau}{\tau_0}\frac{dy^+}{du^+} - 1; \tag{33}$$

substituting appropriately, Van Driest's analysis leads to

$$\epsilon_{m,r} = \frac{1}{2}\left(1+4\frac{\tau}{\tau_0}K^2y^2\left[1-\exp\left(-\frac{y}{A}\right)\right]^2\right)^{\frac{1}{2}} - \tfrac{1}{2}. \tag{34}$$

In the middle region of the tube, this expression reduces to

$$\epsilon_{m,r} = 2\left(\frac{\tau}{\tau_0}\right)^{\frac{1}{2}} Ky; \tag{34b}$$

like the Von Kármán result, it gives a zero value at the centre and is thus unacceptable.

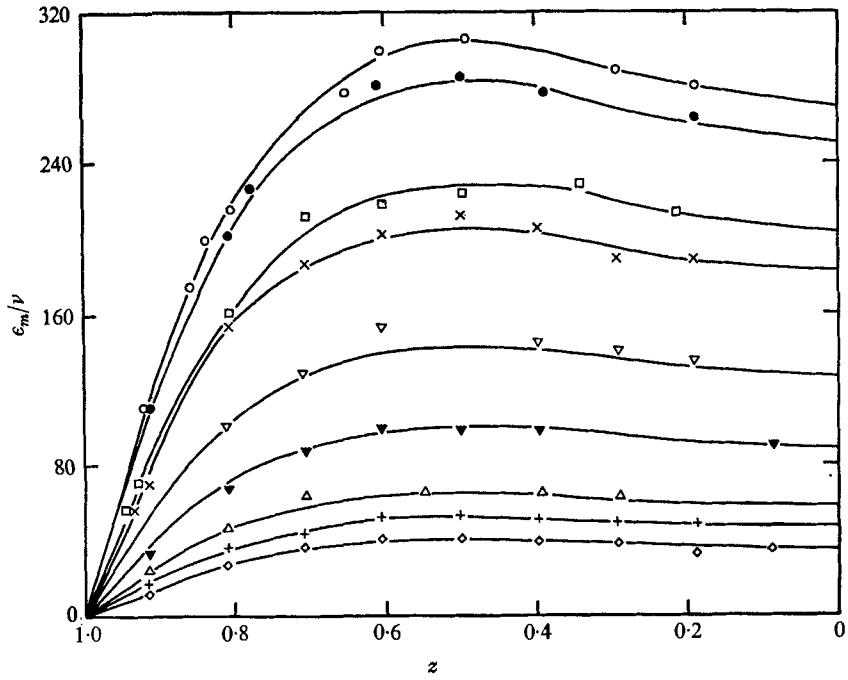

FIGURE 2. Radial eddy diffusivity of momentum. Experiment: ○, R = 155,000; ●, 144,500; □, 115,000; ×, 102,000; ▽, 68,500; ▼, 45,500; △, 32,600; +, 24,800; ◇, 18,500. Theory, equation (36): ——.

However, an expression for $\epsilon_{m,r}$ in the middle region was suggested by Reichardt (1951), which gives good agreement with experiment, and a finite value for $\epsilon_{m,r}$ at the centre of the tube. This is

$$\frac{\epsilon_{m,r}}{\nu} = \frac{0{\cdot}4}{3} r_0^+ \left[0{\cdot}5 + \left(\frac{r^+}{r_0^+}\right)^2\right]\left[1 - \left(\frac{r^+}{r_0^+}\right)^2\right]. \tag{35}$$

Van Driest's expression can be modified to become Reichardt's middle region expression for larger values of y^+ by equating (34*b*) and (35) and substituting into (34*a*). Thus, for all values of y^+, the radial eddy diffusivity of momentum is given by

$$\frac{\epsilon_{m,r}}{\nu} = \frac{K'}{2}\left\{1 + \frac{0{\cdot}16}{9} r_0^{+2}\left[1 - \left(\frac{r^+}{r_0^+}\right)^2\right]^2\left[1 + 2\left(\frac{r^+}{r_0^+}\right)^2\right]^2\left[1 - \exp\left(-\frac{y^+}{26}\right)\right]^2\right\}^{\frac{1}{2}} - \frac{K'}{2}, \tag{36}$$

where the value $A = 26$ given by Van Driest is used.

Equation (36) is used in both the sublayer and mainstream. In the sublayer it is indistinguishable from the eddy diffusivity expression of Deissler (1955, (27)). There is thus no discrepancy between $\epsilon_{m,r}$ and the velocity profile in the sublayer. In the mainstream, however, the velocity profile may also be deduced from (36) and (33). But such a procedure does not give a velocity profile, which is in as good agreement with experiment as the two part model described above.

In (36) the factor K' has been introduced to give better agreement with experiments, which are described below. The factor K' was determined as (*a*) $K' = 1$ for Reynolds numbers less than 40,000, (*b*) $K' = 1{\cdot}15$ for Reynolds numbers greater than 40,000. Figure 2 shows the agreement between (36) and experiment.

(vi) *Radial eddy diffusivity of mass*

The main purpose for this work is to determine the ratio of the radial eddy diffusivity of mass to that of momentum. The prediction of the ratio of the eddy diffusivity of heat to that of momentum has been the subject of much investigation. Since, as mentioned above, there are some arguments to suggest that the analogy between heat transfer and mass transfer would be a good one, it seemed justifiable as a beginning to take expressions for the ratio of $\epsilon_{d,r}$ to $\epsilon_{m,r}$ from the work on the ratio $\epsilon_{h,r}$ to $\epsilon_{m,r}$.

Much experimental work has shown that the Reynolds analogy is of restricted validity, for example, the work of Fage & Falkner (1932), Corcoran & Page (1952) and Sleicher (1958) for heat transfer in air, and of Isakoff & Drew (1951) for liquid metals. In the light of such results, attempts have been made to modify the Reynolds analogy to include the influence of the physical properties of the fluid. An expression for the ratio of $\epsilon_{h,r}$ to $\epsilon_{m,r}$ proposed by Jenkins (1951) has been used in heat transfer calculations with some success. In the Prandtl concept, the eddy moves with constant velocity and temperature, so that the temperature fluctuation t' is equal to $l(dt/dy)$, and

$$\epsilon_{h,r} = lv, \tag{37}$$

where v is the eddy velocity. Jenkins considered that eddies change their energy and momentum while moving as a result of thermal conductivity and molecular viscosity, so that $\epsilon_{h,r}$ is reduced; also, not all the heat, which the eddy had in the original layer, is given up to the second layer; a lesser amount is given up, and

$$\epsilon_{h,r} = lv\frac{t_f - t_i}{l(dt/dy)}, \tag{38}$$

where t_i is the initial temperature of the eddy, and t_f the temperature on disintegration. The temperature of the moving eddy is estimated by assuming it to be a sphere of radius equal to the mixing length, whose surface temperature varies linearly with time. For such a model, Carslaw & Jaeger (1948) gave the average temperature of the sphere at time T as

$$t - t_i = \frac{dt}{dy}\left\{\left(T - \frac{l^2}{15\alpha}\right) + \frac{6l^2}{\pi^4\alpha}\sum_{n=1}^{\infty}\frac{1}{n^6}\left[1 - \exp\left(-\frac{n^2\pi^2\alpha}{\rho}\right)\right]\right\}, \tag{39}$$

where α is the thermal diffusivity. When the eddy reaches the second layer a time interval l/v has elapsed, and $t_f - t_i$ may be obtained from (39) by substitution

of this quantity for T. Jenkins further considers that the momentum transfer from the eddy during its motion should be given by an equation of the same form as that of Carslaw & Jaeger. Thus

$$\epsilon_{m,r} = \frac{2(lv)^2}{\nu}\left\{\frac{1}{15} - \frac{6}{\pi^6}\left(\frac{lv}{\nu}\right)\sum_{n=1}^{\infty}\frac{1}{n^6}\left[1-\exp\left(-\frac{n^2\pi^2\nu}{\rho v}\right)\right]\right\}, \tag{40}$$

and the ratio of $\epsilon_{d,r}$ to $\epsilon_{m,r}$ follows.

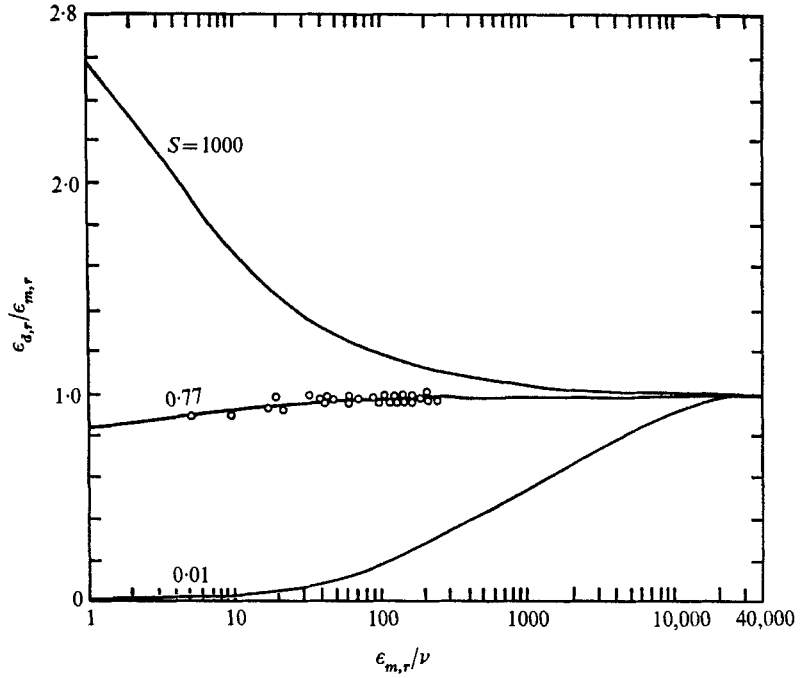

FIGURE 3. Ratio of radial eddy diffusivity of mass to radial eddy diffusivity of momentum. ——, Jenkins's theory, equation (41); O, experimental measurements, S = 0·77.

By replacing the Prandtl number in Jenkins expression by the Schmidt number, and α by D, an expression relating $\epsilon_{d,r}$ to $\epsilon_{m,r}$ is obtained, thus

$$\frac{\epsilon_{d,r}}{\epsilon_{m,r}} = S\left\{\frac{1-\dfrac{90}{\pi^6}\dfrac{lv}{D}\displaystyle\sum_{n=1}^{n=\infty}\frac{1}{n^6}\left[1-\exp\left(-\frac{n^2\pi^2 D}{lv}\right)\right]}{1-\dfrac{90}{\pi^6}\dfrac{lv}{\nu}\displaystyle\sum_{n=1}^{n=\infty}\frac{1}{n^6}\left[1-\exp\left(-\frac{n^2\pi^2\nu}{lv}\right)\right]}\right\}. \tag{41}$$

In this expression the denominator may be related to $\epsilon_{m,r}$, and the ratio may be thus expressed as a function of $\epsilon_{m,r}$. This is shown in figure 3.

The model of a spherical eddy, which loses heat and momentum during its motion between layers, was also used by Azer & Chao (1960), who took the surface coefficient of heat transfer from laminar boundary-layer theory for a flat plate. In the Azer & Chao expression, the ratio of eddy diffusivities is related to the Prandtl number and Reynolds number of the flow, rather than to the Prandtl number and the local value of $\epsilon_{m,r}$. An analysis of heat transfer in concentric

annuli given by Quarmby & Anand (1969) showed, surprisingly, that the results given by the Jenkins expression, and the Azer & Chao expression, are in very close agreement. In this work, it was first intended to try out proposals for the ratio of $\epsilon_{d,r}$ to $\epsilon_{m,r}$. The results achieved with the Jenkins expression were satisfactory, however.

3. Calculations

The choice of r_0^+ as the basic parameter determines the Reynolds number; since R may be written as

$$R = -\frac{4}{r_0^+}\int_0^{r_0^+} u^+(y^+ - r_0^+)\,dr^+, \tag{42}$$

and this may be evaluated by substitution of u^+ evaluated from (26) and (29). The values of r_0^+, corresponding to the Reynolds numbers considered in this work, are given in table 1. The eigenvalues of (11) were found by numerical integration, using a Runge–Kutta method and a Newton–Raphson iteration scheme to allow an accurate determination. The constants were evaluated also by Runge–Kutta integration from either (15) or (23), as appropriate. These calculations were made for exactly those Reynolds numbers for which the experiments were performed. For diffusion from the point source in the centre of the tube the Reynolds numbers were 20,800, 33,000, 67,000, 82,000, 101,000, 119,000 and 130,000. For diffusion from the ring source the Reynolds numbers were 20,800 and 44,700.

r_0^+	R	r_0^+	R
600	20,778	2,000	81,944
900	33,027	2,405	101,076
1,180	44,741	2,780	119,132
1.670	66,902	3,000	129,858

TABLE 1. Relationship between Reynolds number and the parameter r_0^+.

The measured initial profile for the centre point source was described by fitting an equation of the form

$$\theta_i = \exp\left[a_0 + a_1\left(\frac{r}{r_0}\right)^2\right], \tag{43}$$

whilst for the ring source the measured initial profile was described by a polynomial as

$$\theta_i = \sum_{n=0}^{n=6} a_n\left(\frac{r}{r_0}\right)^n. \tag{44}$$

The eigenvalues for the ring source for $R = 20{,}800$ and 44,700 are, of course, the same as for the centre-point source. The constants are evaluated from (44). If the ring source is treated by superposition, the constants are evaluated from (23), rather than from (15).

Use of the constants and eigenvalues thus obtained allows the non-dimensional

profile to be calculated from either (16) or (25), for any values of x^+ and r.† A comparison with the experiment and measured concentration profiles would show whether the description of $\epsilon_{d,r}$ and the velocity profile is correct.

4. Experimental investigation

The following experimental investigation was conducted to provide a test of the analysis described.

(i) *Experimental apparatus*

Measurements of the velocity profile and concentration profile were made in fully developed turbulent flow of air in a plain brass tube. The tube was 3·875 in. inside diameter, with a 0·062 in. wall thickness. The total length of the tube was

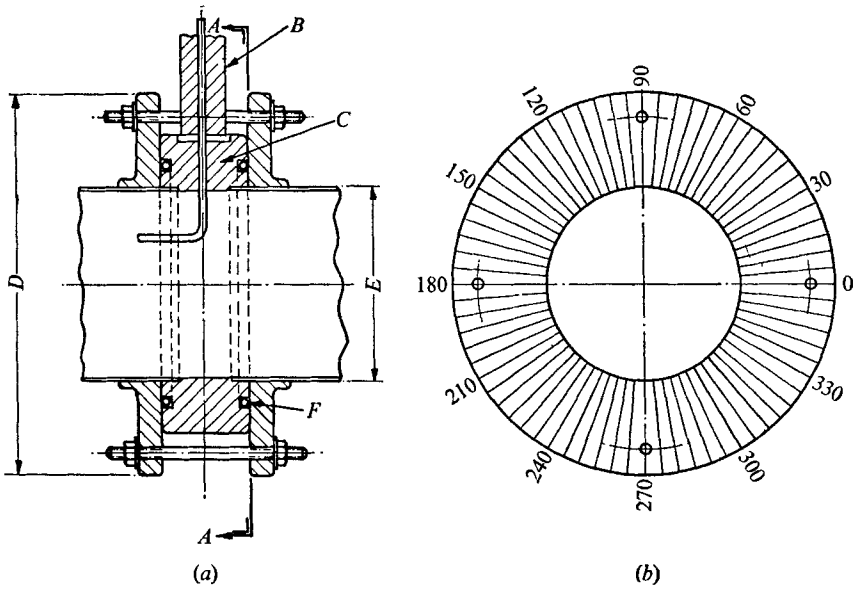

FIGURE 4. Detail of traversing gear and pitot sampling tube. (*a*) *A*, Section on *A*–*A* shown in (*b*); *B*, traversing gear mounted on block *C* is free to rotate when nuts on studs are made loose; *D*, 8 in. diameter. *E*, 4 in. diameter; *F*, $\frac{1}{4}$ in. diameter 'O' ring grooves for air seal.

42 ft 9 in., of which 19 ft 3 in. was the developing section, and 23 ft 6 in. the working section. Filtered clean air was supplied by a fan, and Reynolds numbers up to 155,000 could be obtained.

Pressure taps along the tube allowed the wall shear stress to be determined in the working section. Air temperatures in the working section were measured by thermocouples. The mass flow rate was determined very accurately by the velocity profile near the exit of the tube. Velocity profiles were measured by rectangular-mouthed pitot tubes 0·010 in. wide, made from stainless steel hypodermic tube.

† The constants and eigenvalues were determined to six significant figures and the complete tables are too lengthy to be given here. They may be obtained from either author.

The gas sampling tubes were identical to the pitot tubes. Both kinds of tube were held in mild steel circular traversing blocks. These blocks could be rotated about the tube axis, and were fitted with a micrometer traversing gear. The arrangement is shown in figure 4. It allowed velocity and concentration measurements to be made at any radial or tangential position at each traversing station. The eleven traversing stations were positioned at 4, 11, 20, 29, 38, 62·5, 102·5,

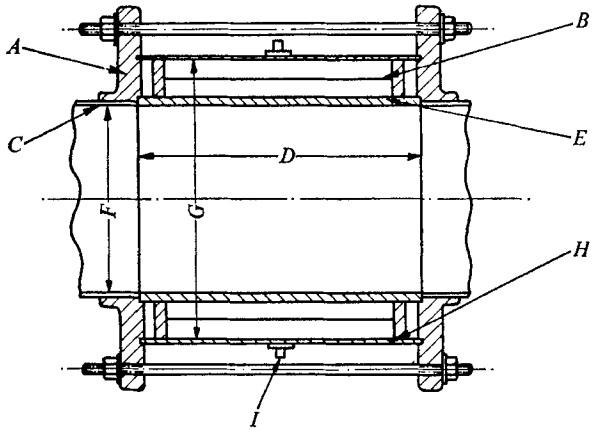

FIGURE 5. Detail of ring source. *A*, flange; *B*, brass wire gauze. *C*, brass tube; *D*, $5\frac{3}{4}$ in.; *E*, Vyon porous plastic; *F*, $3\frac{7}{8}$ in. diameter; *G*, 6 in. diameter; *H*, Perspex outer tube; *I*, nitrous oxide inlets.

142·5, 182·5, 222·5 and 274·5 in. from the source respectively. Pressure measurements were made using a Cassella micrometer, which is accurate to 0·01 mm. The nitrous oxide gas samples were analyzed with a Hilger–Watts infrared gas analyser. When calibrated, this is accurate to 1 % of full-scale deflexion.

The centre-point source was made very simply from stainless steel hypodermic tubing 0·0425 in. outside diameter, and 0·030 in. inside diameter. A right angle bend in this tube allowed the mouth to be positioned accurately in the centre of the working section. The mouth pointed downstream rather in the manner of a backward facing pitot tube. The ring source is shown in figure 5. When assembled, the porous plastic wall was machined to size, so that it was perfectly flush with the wall of the working section.

Nitrous oxide gas, Schmidt number = 0·77, was supplied to each of these sources from a storage bottle *via* a pressure reduction valve and needle valve, which allowed a fine control of the amount of gas injected. The volume flow of nitrous oxide was measured by calibrated rotameter gauges. These were accurate to $\pm\frac{1}{2}$ %. The bulk concentration was calculated from this measurement.

(ii) *Experimental measurements*

In some preliminary experiments, measurements of the wall shear and velocity profile at different axial and tangential positions confirmed that the development length of about 80 diameters was sufficient to ensure fully developed axisym-

metric turbulent flow throughout the working section. The friction factors, and the $u^+ \sim y^+$ results calculated from these measurements, were in very good agreement with results in the literature.

The radial eddy diffusivity of momentum $\epsilon_{m,r}$ was evaluated from (33) for several values of Reynolds numbers in the range considered. The axial position taken for this evaluation was $x^+ = 31$. The slope du^+/dy^+ was evaluated from the measured velocity profile by use of numerical differentiation formulae given by Lanczos (1958). Since the differentiation of empirical functions is a rather uncertain process the results were checked by the Douglas–Avakian

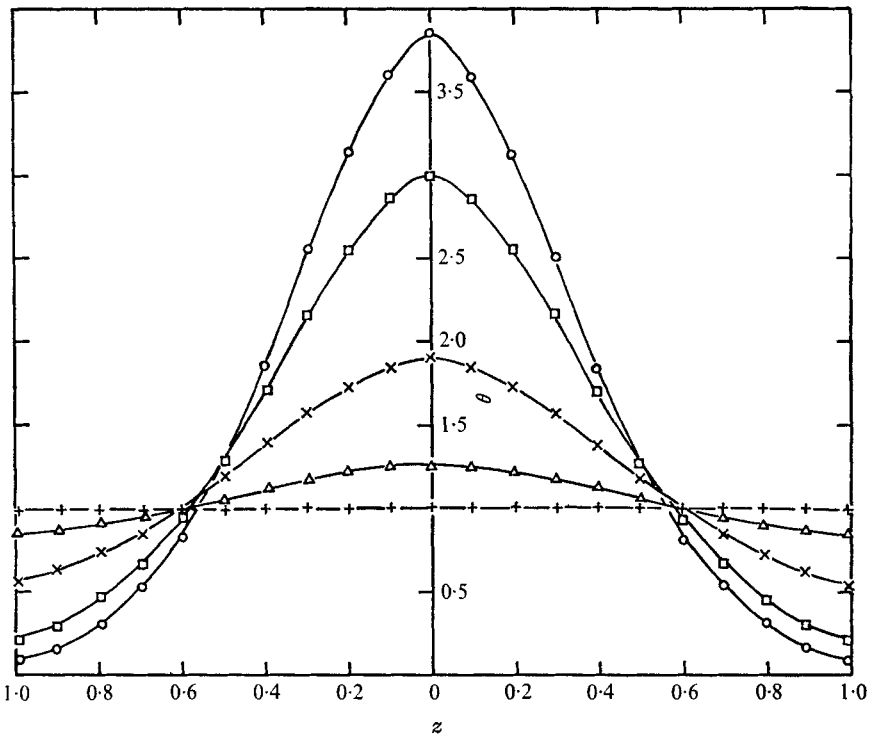

FIGURE 6. Theoretical and experimental concentration profiles for the centre point source. R = 20,800. Theory, equation (16): ——. Experiment, x^+: ○, 13·96; □, 18·60; ×, 31·00; △, 51·66; +, 113·64.

method. The results are shown in figure 2, where a comparison is made with the proposed expression for $\epsilon_{m,r}$, equation (36). The values given for K' were determined from these experiments.

With the centre point source in position there would be a disturbance of the velocity profile. Measurements of the velocity were made at the first axial position downstream of the source. It was established that any disturbances due to the source were no longer detectable. Accordingly, θ_i could be measured there, and the assumption of a fully developed turbulent velocity profile was still valid.

With the centre point source, measurements of the concentration profile were made at each axial position for each of the seven Reynolds numbers listed above.

With the ring source, measurements were made at each axial position for the two Reynolds numbers listed above. The axisymmetry of the concentration profiles was checked by taking measurements at several tangential positions. It was found to be perfectly satisfactory. The high density of the nitrous oxide

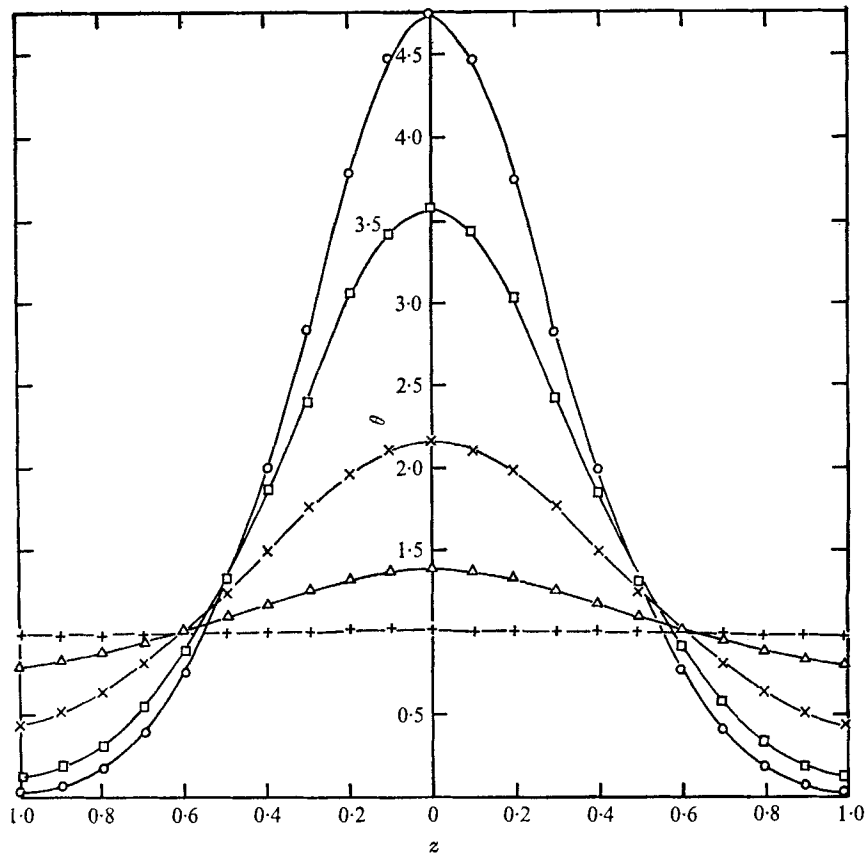

FIGURE 7. Theoretical and experimental concentration profiles for the centre point source. R = 129,900. Theory, equation (16): ——. Experiment, x^+: ○, 13·95; □, 18·60; ×, 31·00; △, 51·66; +, 113·64.

tracer gas (1·5 times that of air) did not lead to asymmetry, since the amount of gas was small. Bakke & Leach (1965) have shown that buoyancy has a negligible effect in turbulent diffusion in a horizontal flow, if the layering number is greater than 10. In these experiments the minimum value of the layering number was 450.

5. Comparison between theory and experiment

Some results for diffusion from a point source at the centre of the tube are shown in figures 6–8. The measured concentration profiles at various axial positions are shown in figure 6 for the lowest Reynolds number studied,

$R = 20{,}800$, and in figure 7 for the highest Reynolds number, $R = 130{,}000$. Figure 8 shows the axial development of the concentration profile for $R = 20{,}800$. In each of these the agreement between experiment and the analysis is most satisfactory. Equally good agreement was found for the five other Reynolds numbers considered.

Figure 9 shows the measurements for $R = 20{,}800$, obtained for the ring source at $x^+ = 0$, which corresponds to the downstream edge of the source, and at

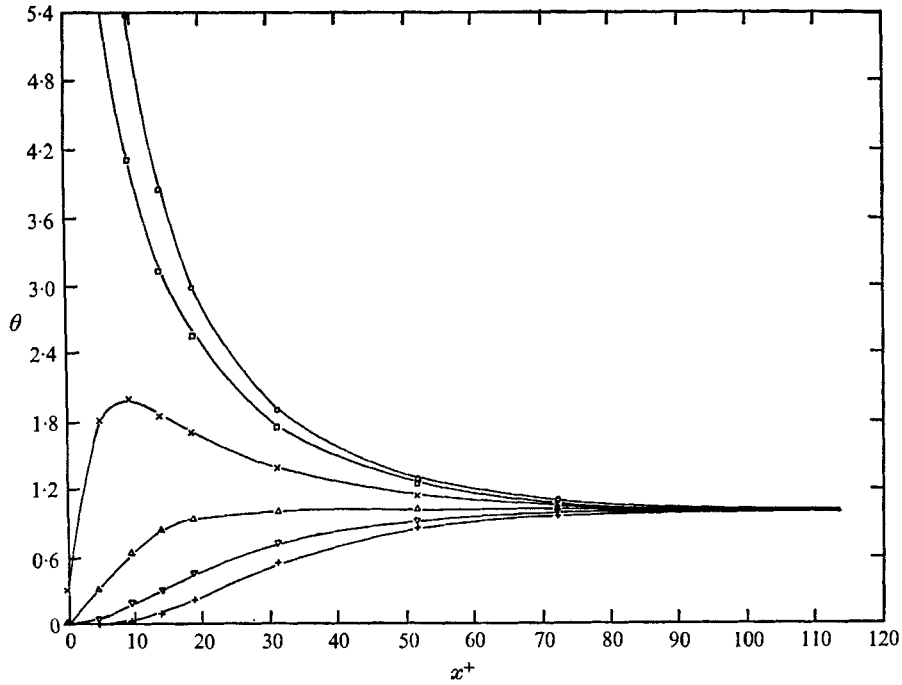

FIGURE 8. Axial development of the concentration profiles for the centre point source. $R = 20{,}800$. Theory, equation (16): ——. Experiment, z: ○, 0·000; □, 0·198; ×, 0·396; △, 0·594; ▽, 0·792; +, 0·990.

$x^+ = 4{\cdot}15$. The agreement between the experiments and the superposition theory at the downstream edge of the source is quite satisfactory. The measured concentration profiles at the other axial positions are shown in figure 10. In these cases, the superposition analysis and analysis using a polynomial to describe the initial profile are indistinguishable, and both are in satisfactory agreement with experiment. Equally good agreement was found for $R = 44{,}700$. It may be noted that, in the experimental results presented, the non-dimensional concentration profile attained the value unity for large x^+. This result establishes the accuracy of the measurement of concentration, and also that of the measurement of the amount of gas injected. If either of these were inaccurate, an anomalous result would have been obtained: the average value of θ across the tube would not have been unity.

In addition to providing a test of the analyses and the validity of the assumptions made concerning the ratio of the radial eddy diffusivity of mass to that of

momentum, the measured concentration profiles may also be used to give a more direct determination of $\epsilon_{d,r}$. Thus, (3) may be written

$$\frac{\epsilon_{d,r}}{\nu} = \frac{r_0^+ \int_0^z u^+ z \frac{\partial \theta}{\partial x^+} dz}{z \frac{\partial \theta}{\partial z}} - \frac{1}{S}. \tag{45}$$

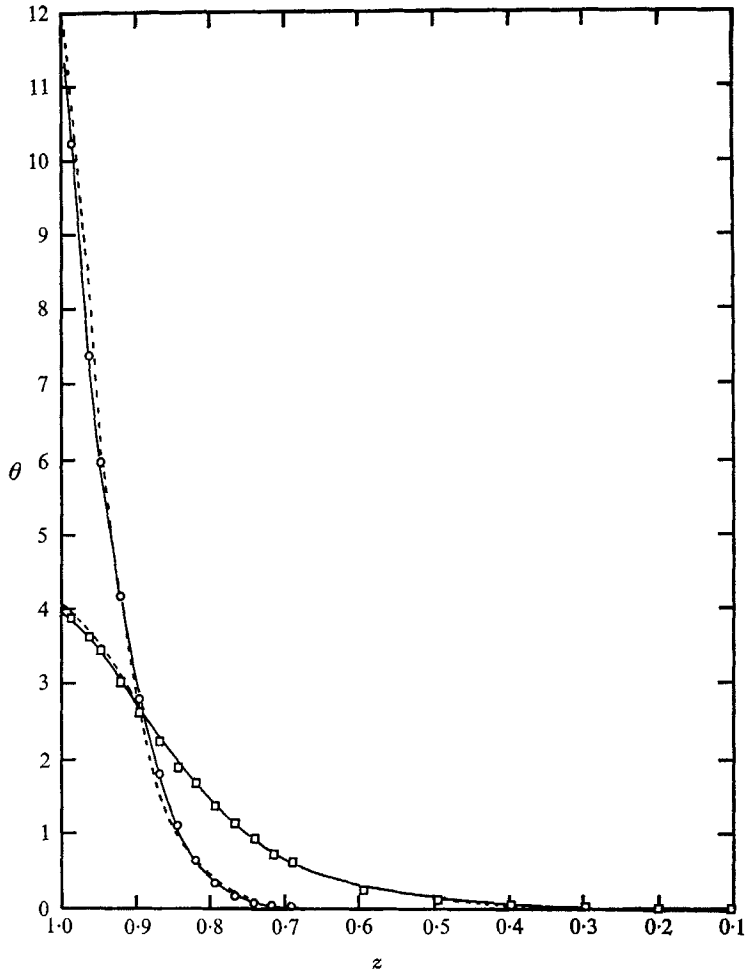

FIGURE 9. Theoretical and experimental concentration profiles for the ring source at low x^+. R = 20,800. Experiment, x^+: ○, 0·00; □, 4·13. – – – –, constant mass flux source theory; ——, polynomial fit theory.

In (45), the slopes $\partial\theta/\partial x^+$ and $\partial\theta/\partial z$ were evaluated from the measured concentration profiles by use of the numerical differentiation formulae. The same methods were used as in the mentioned evaluation of $\epsilon_{m,r}$, and the same axial position as before, $x^+ = 31$, was taken for determining $\epsilon_{d,r}$. Figure 11 shows the results of determining $\epsilon_{d,r}$ for the seven Reynolds numbers considered. The

measurements are compared in figure 11 with the description of $\epsilon_{d,r}$ given by using (36) for $\epsilon_{m,r}$ and (41), the expression for the ratio of $\epsilon_{d,r}$ to $\epsilon_{m,r}$. The agreement is quite satisfactory. These measurements may be expressed as the ratio of $\epsilon_{d,r}$ to $\epsilon_{m,r}$. A comparison with Jenkins expression is shown in figure 3.

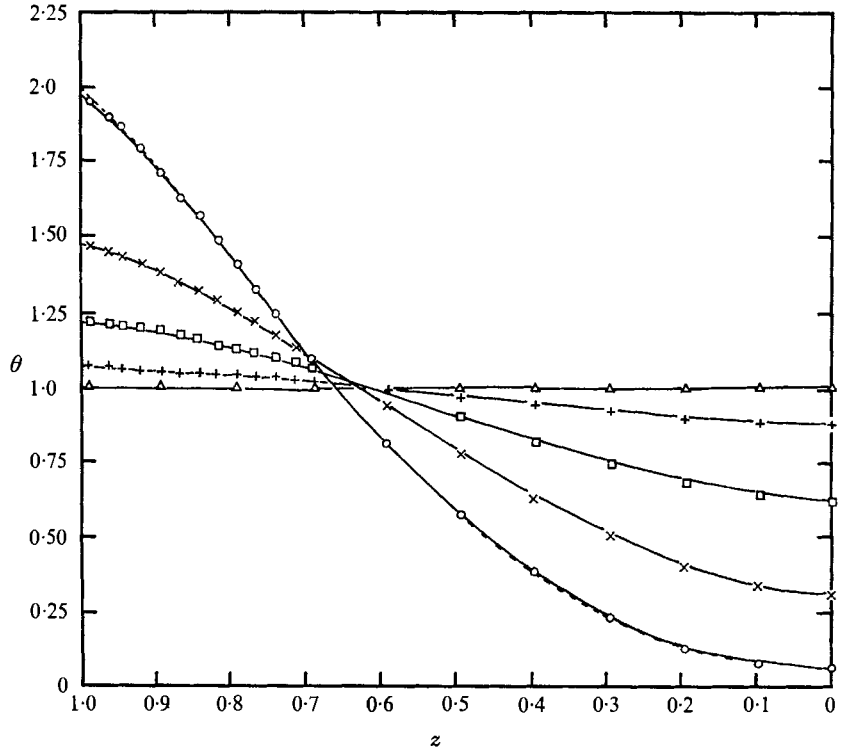

FIGURE 10. Theoretical and experimental concentration profiles for the ring source. R = 20,800. Experiment, n^+: ○, 13·43; ×, 22·73; □, 35·13; +, 55·79; △, 117·77. – – – –, constant mass flux source theory; ——, polynomial fit theory.

A comparison of the present results with previous work is not easy, since, as mentioned, some of the earlier investigations used average values for $\epsilon_{d,r}$. Average values may be obtained from the present results by integration of $\epsilon_{d,r}$ across the tube, and a comparison may be made with the results of Towle & Sherwood (1949). Towle & Sherwood carried out experiments in a fully developed turbulent air stream, in which hydrogen and carbon dioxide were introduced at the axis of a plain tube. Measurements of the concentration profile were made over the central third of the diameter for the Reynolds numbers from 12,000 to 180,000. The results were then interpreted in terms of the calculated average values of the eddy diffusivity, which were obtained by comparing the data with an adaptation of an analysis given by Wilson (1904). A comparison between the present results and Towle & Sherwood's results is given in table 2. The agreement is satisfactory.

Other results for an average $\epsilon_{d,r}$ have been obtained by Schlinger & Sage (1953). Schlinger & Sage injected natural gas through a pipe of 1 in. diameter placed

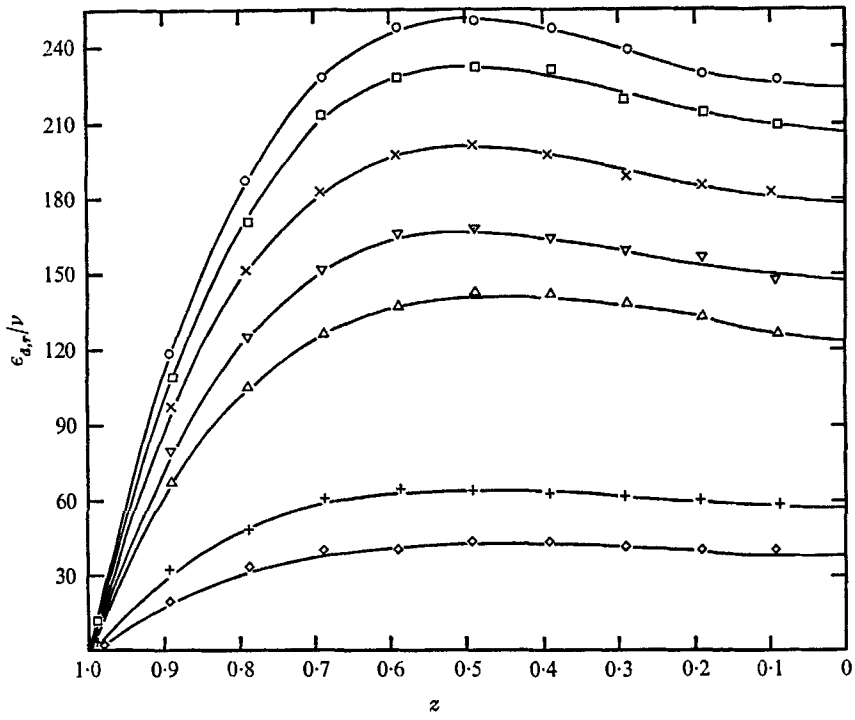

FIGURE 11. Radial eddy diffusivity of mass. Theory, equations (36), (41): ——. Experiment: ○, R = 129,900; □, 119.100; ×, 101,000; ▽, 81,950; △, 66,900; +, 33,000; ◇, 20,800.

Reynolds number	Average $\epsilon_{d,r}$	Average $\frac{\epsilon_{d,r}}{\nu}$	$\int_0^{r_0^+} \frac{\epsilon_{d,r}}{\nu} \frac{dr^+}{r_0^+}$ from (36)
	Towle & Sherwood (1939)		
	cm²/s	at 70° F	
12,200	4·2— 5	27·6— 35·0	20·6
24,600	7 — 7·3	46·1— 48·2	41·0
44,000	11·9—13	78·5— 85·6	80·9
57,400	13 —13·9	85·7— 91·6	103
91,000	20·3—27	134 —178	159
119.000	24 —27·9	158 —184	193
180,000	36·5—45	241 —297	278
	Schlinger & Sage (1953)		
	ft²/s × 10³	at 80° F	
44,000	3·870	21·1	80·9
88,000	9·500	51·7	159
176,000	23·0	125	275

TABLE 2. Comparison of present results for the average radial eddy diffusivity of mass with previous work.

at the axis of a pipe 4 in. in diameter. A comparison with their results and the present results is given in table 2. The agreement is not good. It is felt that the results of Schlinger & Sage are not really appropriate to the present case, because of the disturbance of the large injector in the turbulent air stream.

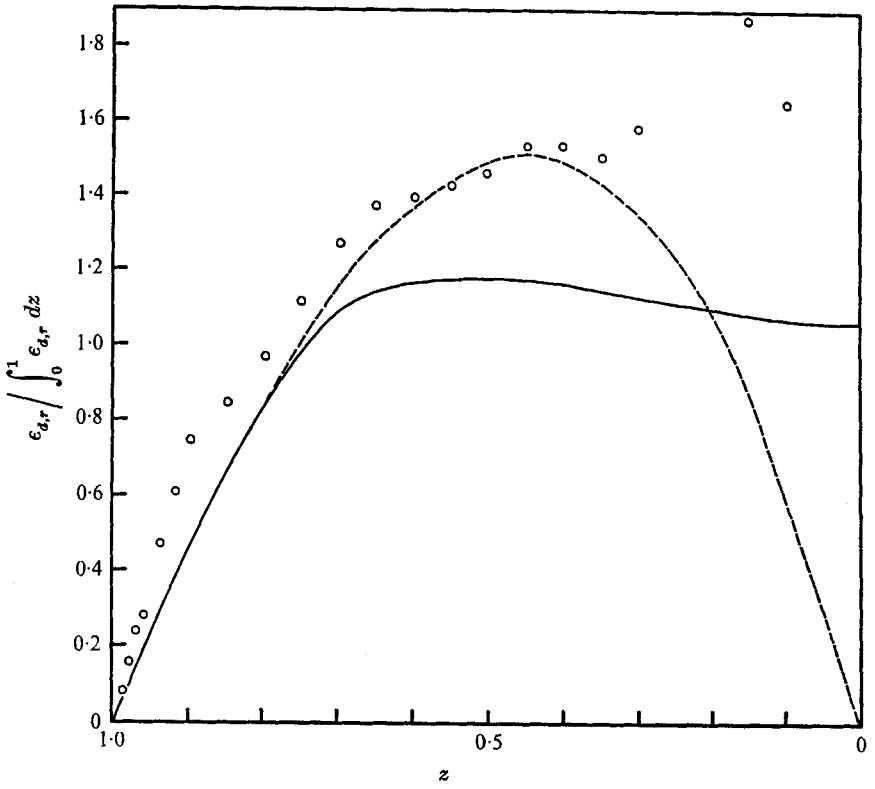

FIGURE 12. Various assumptions about the radial eddy diffusivity of momentum. O, Taylor (1954), $z/f(z)$; – – – –, similarity hypothesis, Von Kármán (1930); ——, equation (36).

Taylor (1954) gave results for the dispersion of matter in turbulent flow in a pipe, where the concentration of brine was determined by measurement of the electrical conductivity. The value of the virtual coefficient of diffusion was obtained from the experimental results, but this is not comparable with values for $\epsilon_{d,r}$. To compare the present results with Taylor's work, we need to calculate the eddy diffusivity function he assumed by use of (2), and the table of values of z and $f'(z)$, which he gave. Equation (2) may be written

$$\epsilon_{m,r}/\nu = r_0^+ z/f'(z), \tag{46}$$

and thus be linked to the Reynolds number by table 1. Taylor linked u^+ with the Reynolds number by an empirical equation for the friction factor. The results on table 1 are in perfect agreement with the friction factor equation, and are simpler to use here. From the table given by Taylor, the values of $z/f'(z)$ were calculated, and these values normalized with respect to their average value are

shown in figure 12. We cannot deduce from the Taylor table whether $\epsilon_{m,r}$ becomes zero or not at $z = 0$, but the general shape of the result agrees with (36). However, the values for $\epsilon_{m,r}/\nu$, from (46), are less by about one-third. Estimating the average value of $z/f'(z)$ from figure 12 gives an average value for $\epsilon_{m,r}/\nu$ at $R = 44{,}000$ as 56·6, whilst at $R = 119{,}000$ we get $\epsilon_{m,r}/\nu = 133$. These figures also give us Taylor's values of $\epsilon_{d,r}$, since Taylor assumed $\epsilon_{d,r} = \epsilon_{m,r}$. Figure 12 also shows a normalized result for $\epsilon_{m,r}$, according to both (36) and the Von Kármán similarity hypothesis.

6. Conclusion

Good agreement has been found between the predictions of the analysis presented for mass transfer into a fully developed turbulent flow in a plain tube and careful experiments using nitrous oxide, Schmidt number = 0·77, as a tracer gas in air. The range of the investigation covered Reynolds numbers from 20,000 to 130,000, and good agreement was found throughout this range. The agreement was equally good whether the mass transfer was mainly taking place in the central core of the flow or in the wall region. It is concluded, that the description of the velocity and eddy diffusivity profiles used in the solution of the diffusion equation, is accurate.

The formulation used for the solution of the diffusion equation for fully developed turbulent flow in a plain tube may be summarized as follows. The velocity profile is described by a two-part model of a sublayer and mainstream. In the sublayer, Deissler's (1955) expression is used and, in the mainstream, the velocity is deduced from Von Kármán's (1930) similarity hypothesis. The radial eddy diffusivity of momentum is given by an expression, based on the work of Van Driest (1956) and Reichardt (1951), in which the influence of the wall on the turbulent fluctuations is taken into account. This expression gives a finite value for eddy diffusivity at the centre of the tube. The radial eddy diffusivity of mass is obtained from that of momentum by a ratio based on the work of Jenkins (1951) which takes account of the fluid properties.

In addition to the evidence provided by the comparison of the theoretical and experimental concentration profiles, accurate direct measurements were obtained of the ratio of the eddy diffusivity of mass to that of momentum. The agreement with Jenkins expression for Schmidt number = 0·77 was satisfactory, and gives added confirmation to the above conclusion. The results determining the eddy diffusivity of mass as a function of radial position are an improvement on previous work on this subject, since it is usually assumed to have a constant value for a given flow.

The theoretical results obtained for axisymmetric diffusion, and the experimental techniques developed in this investigation, establish a firm base, from which the non-axisymmetric situation may be studied. Also, the present formulation of the solution of the diffusion equation for fully developed turbulent flow in a plain tube may be used to give accurate solutions for axisymmetric situations, which are different from the ones considered here.

REFERENCES

AZER, N. Z. & CHAO, B. T. 1960 *Int. J. Heat Mass Transfer*, **1**, 121.

BAKKE, P. & LEACH, S. K. 1965 *Appl. Sci. Res.* A **15**, 97.

CORCORAN, W. H. & PAGE, F. 1952 *Ind. Engng Chem.* **44**, 410.

DEISSLER, R. G. 1955 *NACA TM* 1210.

ELROD, H. G. 1957 *J. Aero. Sci.* **24**, 468.

FAGE, A. & FALKNER, V. M. 1932 *Proc. Roy. Soc.* A **135**, 685.

ISAKOFF, S. E. & DREW, T. B. 1951 *General Discussion on Heat Transfer*. I. Mech. E.

JENKINS, R. 1951 *Proc. Heat Transfer and Fluid Mechanics Inst.* Stanford, California.

LANCZOS, C. 1957 *Applied Analysis*. London: Pitman.

LEUNG, E. Y., KAYS, W. M. & REYNOLDS, W. C. 1963 *Int. J. Heat Mass Transfer*, **6**, 445.

PRANDTL, L. 1933 *Z. Ver. dt. Ing.* **77**, 105.

QUARMBY, A. 1969 *J. mech. Engng Sci.* **2**, 45.

QUARMBY, A. & ANAND, R. K. 1969 *Chem. Engng Sci.* **24**, 171.

REICHARDT, H. 1951 *ZAMM*, **31**, 208.

SCHLINGER, W. G. & SAGE, B. H. 1953 *Ind. Engng Chem.* **45**, 659.

SHERWOOD, T. K. & WOERTZ, B. B. 1939 *Am. Inst. Chem. Eng.* **35**, 519.

SLEICHER, C. A. 1958 *Trans. Am. Soc. mech. Engrs*, **80**, 693.

SPARROW, E. M., HALLMAN, J. M. & SEIGEL, R. 1957 *Appl. Sci. Res.* A **7**, 37.

STOKES, G. G. 1851 *Trans. Camb. Phil. Soc.* **9**, 73.

TAYLOR, G. I. 1954 *Proc. Roy. Soc.* A **223**, 446.

TOWLE, W. L. & SHERWOOD, T. K. 1939 *Ind. Engng Chem.* **31**, 457.

VAN DRIEST, E. R. 1956 *J. Aero. Sci.* **23**, 1007.

VON KÁRMÁN, T. 1930 *Proc. 3rd Int. Congr. Appl. Mech.* **1**, 85.